OXFORD UNIVERSITY PRESS | FEMS Microbiology Letters

http://mc.manuscriptcentral.com/fems

Lipopolysaccharide surface structure does not influence IcsA polarity.

Journal:	*FEMS Microbiology Letters*
Manuscript ID:	Draft
Manuscript Type:	Research Letter
Date Submitted by the Author:	n/a
Complete List of Authors:	Doyle, Matthew; The University of Adelaide, Molecular and Cellular Biology Grabowicz, Marcin; Princeton University, Molecular Biology May, Kerrie; Princeton University, Molecular Biology Morona, Renato; The University of Adelaide, Molecular and Cellular Biology
Keywords:	Outer membrane, Bacterial pole, Lipopolysaccharide, Autotransporter, Minicell, Shigella
All articles in FEMS Microbiology Letters are published under one of eight subject sections. Please select the most appropriate subject category for your submission from the drop down list:	Pathogens & Pathogenicity

TITLE: Lipopolysaccharide surface structure does not influence IcsA polarity.

RUNNING TITLE: LPS and IcsA localisation.

AUTHORS:

Matthew Thomas Doyle[a], Marcin Grabowicz[b], Kerrie Leanne May[b], and Renato Morona[a,#]

ADDRESS WORK WAS PERFORMED:

Department of Molecular and Cellular Biology, School of Biological Sciences, University of Adelaide, Adelaide 5005, Australia

AFFILIATIONS:

[a]Department of Molecular and Cellular Biology, School of Biological Sciences, University of Adelaide, Adelaide, Australia

[b]Department of Molecular Biology, Princeton University, Princeton, USA

CORRESPONDING EMAIL: [#]Renato Morona: renato.morona@adelaide.edu.au.

KEY WORDS: Outer membrane, Bacterial pole, Lipopolysaccharide, Autotransporter, Minicell, *Shigella*

ABSTRACT

Shigella species are the causative agents of human bacillary dysentery. These bacteria spread within the lining of the gut via a process termed actin-based motility whereby an actin 'tail' is formed at the bacterial pole. The bacterial outer membrane protein IcsA initiates this process, and crucially, is precisely positioned on the bacterial polar surface. Lipopolysaccharide (LPS) O-antigen surface structure has been implicated as an augmenting factor of polarity maintenance due to the apparent dysregulation of IcsA polarity in O-antigen deficient strains. Due to *Shigellae* having long and short O-antigen chains on their surfaces, it has been proposed that O-antigen chain lengths are asymmetrically distributed to optimize IcsA exposure at the pole and mask exposure laterally. Additionally, it has been proposed that LPS O-antigen restricts IcsA diffusion from the pole by maintaining minimal membrane fluidity. This study utilizes minicells and quantitative microscopy providing data refuting the models of asymmetric masking and membrane diffusion, and supporting a model of symmetric masking of IcsA. We contend that IcsA surface distribution is equivalent between wild-type and O-antigen deficient strains, and that differences in cellular IcsA levels have confounded previous conclusions.

INTRODUCTION

Shigella species such as *Shigella flexneri* are human specific Gram negative bacterial pathogens that are adapted to the invasion of colonic mucosa leading to dysentery (Niyogi 2005; Lima *et al.,* 2015). The outer membrane autotransporter protein IcsA is essential for intra- and inter-cellular spreading of *S. flexneri* in epithelia via the process of actin-based motility (Bernardini *et al.,* 1989; Lett *et al.,* 1989; Goldberg *et al.,* 1995; Kocks *et al.,* 1995; Egile *et al.,* 1999). IcsA is localized to the surface of the old bacterial pole (that which is not derived from the septum of the parent cell) where it binds host cell actin recruiting / polymerizing complexes required for this motility (Egile *et al.,* 1999; Steinhauer *et al.,* 1999; Snapper *et al.,* 2001; Suzuki *et al.,* 2002; May *et al.,* 2008; Valencia-Gallardo *et al.,* 2014). Hence, maintenance of an asymmetrical spatial surface distribution is critical for appropriate functioning of IcsA in all *Shigellae* species. By mechanisms that are yet to be fully elucidated, new IcsA is secreted to the pole after pre-secretion cytoplasmic accumulation (Charles *et al.,* 2001; Rokney *et al.,* 2009). IcsA surface polarity is also refined by the actions of its specific outer membrane protease IcsP which is localised to the new cell pole and the septa of dividing bacteria (Egile *et al.,* 1997; Tran *et al.,* 2013). This opposing distribution results in asymmetric IcsA cleavage and refines IcsA surface polarity (Tran *et al.,* 2013).

Lipopolysaccharide (LPS) structure has also been implicated as a modulating factor in IcsA biogenesis, polarity, and function. Certainly, *S. flexneri* spreading is abrogated upon changes in LPS structure (Sandlin *et al.,* 1995; Sandlin *et al.,* 1996; Hong *et al.,* 1997; Van den Bosch *et al.,* 1997). However, there is disagreement in the literature concerning the specific mechanisms by which LPS effects IcsA. For instance, immunofluorescence microscopy and immunogold electron microscopy studies have reported that IcsA can be found at increased levels along the lateral surface of rough (R-LPS) *S. flexneri* (strains that lack the O-antigen repeat chain component of LPS), as opposed to the refined polar detection

of smooth (S-LPS) wild-type *S. flexneri* (Sandlin *et al.,* 1995; Van den Bosch *et al.,* 1997; Robbins *et al.,* 2001). In explanation, it was proposed that R-LPS strains have higher membrane fluidity (Figure 1A) resulting in easier diffusion of IcsA away from the pole and down the sides of the bacterium (Robbins *et al.,* 2001). However, this is confounded by the realization that LPS O-antigen chains mask detection of IcsA by limiting antibody access (Morona *et al.,* 2003c; Morona *et al.,* 2003b; Morona *et al.,* 2003a). Therefore, the refined polar detection of IcsA observed on *S. flexneri* may not be the complete picture of its actual surface localization. Further complicating is that *S. flexneri* decorates its surface with two modal lengths of O-antigen repeats; short type (^{S}LPS; 11-17 repeats) (Morona *et al.,* 1995) and very long type (^{VL}LPS; 90+ repeats) (Hong *et al.,* 1997) which are regulated by the $WzzB_{SF}$ and $WzzB_{pHS2}$ inner membrane co-polymerases respectively (Morona *et al.,* 1995; Stevenson *et al.,* 1995; Hong *et al.,* 1997). It has been hypothesized on multiple occasions that *S. flexneri* has two types of O-antigen modal lengths to counteract the steric hindrance effect of LPS, whilst retaining protection from host defences and colicins (Morona *et al.,* 2003c; Pugsley *et al.,* 2004; Scribano *et al.,* 2014; Tran *et al.,* 2014). In this model, ^{VL}LPS is required for serum resistance, whereas ^{S}LPS minimizes IcsA masking at the pole such that it can access external actin recruiting complexes (Figure 1B).

Due to the confounding nature of these models (masking, lateral diffusion / membrane fluidity, asymmetric O-antigen chain lengths), the exact effects of LPS on IcsA surface localisation remains enigmatic. This work unravels the IcsA-LPS relationship in *S. flexneri* by first examining whether LPS O-antigen modal chain lengths are asymmetrically distributed in the outer membrane. IcsA localizations in the rough and wild-type membrane are then quantified and directly compared allowing a re-evaluation of the asymmetrical masking and lateral diffusion models. The results obtained challenge current thoughts

concerning the LPS-IcsA relationship and provide further insights into IcsA polar positioning.

MATERIALS AND METHODS

Bacterial strains, plasmids and culture. Lists of strains and plasmids utilized in this study are included in Table 1. *S. flexneri* colonies were grown on Congo Red agar for confirmation of virulence plasmid presence before routine growth in Luria-Bertani (LB) media at 37˚C with shaking. Unless otherwise stated, bacteria were sub-cultured to a log-phase OD600 reading of 0.5 before experimental use. When required, broths were supplemented with the following additives at respective concentrations; tetracycline (10 μg mL^{-1}), kanamycin (50 μg mL^{-1}), and ampicillin (50 μg mL^{-1}).

Construction of *minD* mutant. The *minCDE* locus of *S. flexneri* 2457T was PCR amplified using oligonucleotides minF (gacttgcctcaatataatcc) and minR (tctgtgcgtgggaacagc) that anneal to nt positions 1210181-1210200 and 1208137-1208154 respectively on the 2457T chromosome (Wei *et al.,* 2003). The amplicon was cloned into pGEMT-Easy (Promega) creating pKMRM96 (Table 1). To disrupt the *minD* gene, the kanamycin resistance (Km^R) cassette from pKD4 (Datsenko *et al.,* 2000) was amplified using P1PacI (ccttaattaagtgtaggctggagctgcttc) and P2PacI (ccttaattaacatatgaatatcctccttag) incorporating flanking PacI sites which were used to insert the Km^R cassette into the native PacI site within the *minD* gene in pKMRM96 resulting in pKDMRM161 (Table 2). The *min* locus containing disrupted *minD::*Km^R was then amplified using minF/R and the amplicon used in recombineering mutagenesis of 2457T *minD* genomic copy via the λ red recombinase system (Datsenko *et al.,* 2000).

Antibodies. Polyclonal rabbit anti-IcsA (passenger), rabbit anti-$WzzB_{SF}$, and rabbit anti-$WzzB_{pHS2}$ were produced and validated as described previously (Van den Bosch *et al.,* 1997;

Daniels *et al.,* 1999; Purins *et al.,* 2008). Mouse anti-DnaK monoclonal antibody was from Enzo Life Sciences.

Total bacterial protein samples. 1:50 sub-cultures were grown to log-phase. 5 x 10^8 of log-phase bacteria were collected by centrifugation (16000 x g, 1 min, 4 ˚C), resuspended in 100 µL of SDS-PAGE loading buffer (Lugtenberg *et al.,* 1975), and heated to 100 ˚C for 10 min before SDS-PAGE and immunoblot analysis.

Bacterial IcsA labelling. Immunofluorescence (IF) staining was conducted essentially as described previously (Tran *et al.,* 2013). All solutions were filtered through a 0.2 µm nitrocellulose filter. 10^8 log-phase bacteria were harvested from a 1:50 sub-culture by centrifugation (16000 x g, 2 min, 20 ˚C), resuspended in 3.7 % (v/v) formaldehyde solution (Sigma) in phosphate buffered saline (PBS), and incubated at 20 ˚C for 20 min. Fixed bacteria were washed twice in PBS before resuspension in 100 µL of PBS. 5 µL of the bacteria were spotted onto sterile round coverslips (at the bottom of a 24-well tray) that were pre-treated with 10 % (v/v) poly-L-lysine solution (Sigma) in PBS. Bacteria were centrifuged (775 x g, 5 min, 20 ˚C) and then incubated for 2 h with anti-IcsA diluted 1:100 in PBS containing 10 % (v/v) fetal calf serum (FCS). Bacteria were washed three times with PBS and then incubated for 30 min at 37 ˚C with donkey anti-rabbit Alexa Fluor 488 antibody (Invitrogen) diluted 1:100 in PBS containing 10 % (v/v) fetal calf serum (FCS). Bacteria were washed three more times with PBS before mounting with 20 % Mowiol 4-88 (Calbiochem), 4 mg mL^{-1} *p*-phenylenediamine.

Minicell and whole-cell purification. Separation of minicells and whole-cells was conducted as described previously (Achtman *et al.,* 1979). The minicell strain was sub-

cultured (1:20) until log-phase, or sub-cultured for 16 h to produce stationary phase cultures. A volume of 250 mL bacteria from both log-phase and stationary-phase cultures were pelleted by centrifugation (8,600 x g, 20 min, 4 ˚C;) and washed in 10 mL of buffered saline gelatin (BSG; 0.85 % (w/v) NaCl, 0.03 % (w/v) KH_2PO_4, 0.06 % (w/v) Na_2HPO_4, 100 µg/mL gelatin). Bacteria were pelleted again (20,400 x g, 8 min, 4 ˚C) and resuspended in 2 mL of BSG. Bacteria were layered onto sucrose gradients and centrifuged (3300 x g, 30 min, 4 ˚C). The minicell fraction in the middle of the tube was extracted using a syringe. The whole-cell fraction at the bottom of the tube was also collected and diluted in 50 mM Tris pH 7.5. The minicells were pelleted (20,400 x g, 8 min, 4 ˚C), resuspended in 1 mL of BSG and purified once more on a sucrose gradient as described. The minicells were then re-pelleted (as above) and resuspended in 2 mL of 50 mM Tris pH 7.5. Cell concentrations were normalised on the basis that an OD600 = 1.0 represents 5 x 10^8 whole cells and 2 x 10^9 minicells.

Minicell and whole-cell membrane protein and LPS analysis. As described previously (Achtman *et al.,* 1979), purified minicells and whole-cells were lysed by sonication in 20 mM Tris-HCl pH 8.0, 10 mM NaCl buffer containing 0.1 mg mL^{-1} DNase, 0.1 mg mL^{-1} RNase, and 0.1 mM phenylmethanesulfonyl fluoride. Unbroken cells were removed by centrifugation (5,500 x g, 25 min, 4 ˚C) and the lysate was ultracentrifuged (100,000 x g, 60 min, 4 ˚C). The whole membrane pellet was rinsed with buffer, homogenised in 20 mM Tris-HCl pH 8.0, 10 mM NaCl buffer containing 1 % (v/v) SDS, and incubated on ice for 1 h. This was then ultracentrifuged (as above) and the resulting supernatant collected. Protein content was assessed using a BCA Protein Estimation assay (Pierce). Membrane samples from minicells and whole-cells were standardised to equivalent total membrane protein concentration for protein analysis by immunoblot. For LPS analysis, samples were treated with 0.5 mg mL^{-1}

Proteinase K in SDS-PAGE loading buffer at 56 ˚C for 16 h and analyzed by SDS-PAGE and silver stain.

Microscopy and quantitation. All images of IF labelled bacteria were captured using an Olympus IX-7 Microscope and MetaMorph software (Molecular Devices) with a phase contrast 100 x oil immersion objective and a 1.5 x enlarger. For fluorescence imaging an X-Cite 120Q lamp was used set at high intensity. All live bacterial imaging was conducted on custom made 1 % (w/v) agarose-LB solid media mounts with 37 ˚C incubation. All bacterial IcsA fluorescence images were acquired with 100 millisecond exposures. Fluorescence images for background correction were taken for each experiment. IcsA fluorescence images for presentation were recolored using the ICA LUT in ImageJ such that the full intensity spectrum can be easily observed. MetaMorph line-scan measurement tools were used to quantitate fluorescence intensities across the perpendicular axis of a point-to-point scan. Scans were conducted from pole-to-pole starting from intense pole, with scan width (perpendicular axis) equal to the bacterium (approx. 20 pixels). For each strain under investigation, cumulative scans were conducted of many bacteria (50 bacteria from each independent experiment '*n*') that were without a visible septum, resulting in distribution profiles representative of the population.

RESULTS AND DISCUSSION

Any asymmetry in LPS O-antigen chain lengths would dramatically change the apparent IcsA polarity between S-LPS and R-LPS strains and may allow increased exposure of IcsA at the pole. To investigate LPS asymmetry we constructed an *S. flexneri minD*- strain (MG292; Table 1). MinD (along with MinC and MinE) regulates appropriate positioning for septum formation in bacterial division (Treuner-Lange *et al.,* 2014). Mutants in this system form minicells that result from mislocalized septation at the poles (de Boer *et al.,* 1989). As such, minicells are rich in polar membrane material compared to whole-cells and have been vital for investigations on the polar cytology (Koppelman *et al.,* 2001; Lai *et al.,* 2004). The *minD*- strain behaved as expected with the formation of free minicells and observed polar budding of minicells (Figure 2A). We then purified both whole-cell and minicell populations of this strain based on density and assessed purity microscopically. The whole-cell fraction was 98.9 % pure (one budding minicell observed per 94 bacteria), and whole-cells were not observed in the minicell fraction (Figure 2B).

Upon assessment of extracted membrane protein (Figure 2C), we observed no discernible difference between whole-cells and minicells in the abundance of O-antigen chain length modulators $WzzB_{SF}$ and $WzzB_{pHS2}$. As expected, minicell membranes were more abundant in IcsA than whole-cells showing that minicells represent polar material of the IcsA pole. Additionally, we also observed no differences in the relative abundances of ^{S}LPS and ^{VL}LPS between minicells and whole-cells. This was true for purified populations from both log-phase and stationary phase cultures (Figure 2D). Therefore, these results do not support a model of enhancement of IcsA exposure at the pole due to an asymmetric distribution of LPS O-antigen chain lengths between the pole and lateral surfaces (Figure 1B). Consequently, the previously observed changes in apparent IcsA distributions between S-LPS and R-LPS bacteria must be due to one or more of the effects of symmetrical masking, membrane

fluidity and lateral diffusion, or other factors. It should also be noted here that, to our knowledge, this is the first observation of LPS O-antigen modal length distribution using minicells.

To thoroughly model IcsA distributions and the effects of LPS, we devised methods to quantitate the average IcsA surface population distribution for a given strain removing biases of qualitative assessment and artificial selection of bacteria (see *Materials and Methods*). We first investigated IcsA differences between the wild-type and R-LPS derivative strains (Figure 3A, B, and C). Our R-LPS strain is unable to make O-antigen due to the absence of RmlD which synthesizes dTDP-rhamnose (a precursor sugar for O-antigen synthesis, see Table 1). Unexpectedly, we observed a large increase in IcsA levels in the R-LPS strain relative wild-type (Figure 3A) which had not previously been reported. However, qualitative IcsA surface distributions replicated previous reports with the R-LPS strain displaying higher lateral and bipolar IcsA detection compared to wild-type (Figure 3B). We quantified these distributions (Figure 3C) and found that IcsA surface detection was significantly more intense for the R-LPS strain (Figure C_i; $p = 0.0002$), yet was still highly localized to the old pole (Figure C_{ii}). Direct comparisons of S-LPS and R-LPS IcsA distributions (Figure C_{iii}) revealed that the R-LPS strain had significantly higher placement of IcsA at the new pole, whether assessed relative to the old pole or the mid-cell ($p = 0.0053$ and $p < 0.0001$ respectively). There was no significant change in IcsA old pole localization relative the mid-cell between S-LPS and R-LPS strains.

These data support previous reports that R-LPS strains have an increased propensity for bipolarity and a reduction in polar refinement, yet it is difficult to assess whether this is due to the increase in overall IcsA expression or due to changes in membrane diffusion of IcsA. Therefore we repeated this investigation using strains expressing IcsA from a plasmid (pIcsA; see Table 1). These conditions equalized IcsA levels between S-LPS and R-LPS

strains as shown (Figure 3D). Qualitatively, IcsA surface distributions on R-LPS bacteria again appeared more intense than S-LPS, but had similar overall distributions (Figure 3E). This was recapitulated when quantitated (Figure $3F_i$ and F_{ii}), but unexpectedly, the quotient of these distributions (Figure $3F_{iii}$) did not show any significant shifts in IcsA localization for any point between the poles.

Contrary to the current literature, the results presented in Figure 3 show that upon IcsA cellular levels being equal, IcsA surface distribution remains indistinguishable regardless of the presence of LPS O-antigen on the membrane. This supports the notion that the masking effect of LPS is exerted symmetrically over the surface of *S. flexneri*, and is further supported by our observations of equivalent O-antigen chain lengths between whole and minicells (indicating symmetrical chain length distributions for wild type) presented in Figure 2. Furthermore, since LPS changes do not affect IcsA polarity, it also shows that R-LPS does not consequently increase the fluidity of IcsA molecules in the outer membrane (Figure 1A). Lateral diffusion of IcsA from the pole is either unchanged or does not occur.

It is also interesting that IcsA levels are increased when O-antigen synthesis is blocked. Although previously utilized *S. flexneri* strains were deficient in O-antigen due to varied mutations (Sandlin *et al.,* 1995; Sandlin *et al.,* 1996; Robbins *et al.,* 2001), it is possible that previous attributions of LPS effecting IcsA polarity were due to overlooked changes in cellular IcsA concentration. The reason for this change in IcsA level is uncertain but it is plausible that degradases responsible for normal IcsA turnover are functionally altered in R-LPS strains resulting in higher steady-state levels. Indeed, we have previously shown that periplasmic protease DegP has altered activities with respect to IcsA maintenance in R-LPS *S. flexneri* (Teh *et al.,* 2012). Nevertheless, it is intriguing that increased IcsA levels increase the tendency for abnormal placement of IcsA at the new pole. It has been proffered that cytoplasmic accumulation at the pole seeds initial placement of IcsA (Charles *et al.,*

2001; Rokney *et al.,* 2009) – it is possible that changes in IcsA abundance can influence this accumulation and increase the tendency for off target accumulation. This notion is consistent with the increases of IcsA at the new pole observed in this work (Figure 3C).

In summary, this study reveals that; (i) *S. flexneri* IcsA polarity, and any diffusion of IcsA in the outer membrane, is **not** affected by LPS O-antigen presence, (ii), IcsA is affected by symmetrical masking, (iii) O-antigen chain lengths are symmetrically distributed, and (iv) changes in O-antigen synthesis can deregulate IcsA levels effecting polarity.

FUNDING

This work was supported by the National Health and Medical Research Council (NHMRC) of Australia [Grant number 565526].

ACKNOWLEDGEMENTS

MTD is the recipient of a Doctor of Philosophy scholarship from the University of Adelaide. We thank the Research Centre for Infectious Diseases (RCID) for support during this work. We also thank Elizabeth Ngoc Hoa Tran for critical reading of the manuscript.

REFERENCES

Achtman M, Manning PA, Edelbluth C & Herrlich P (1979) Export without Proteolytic Processing of Inner and Outer-Membrane Proteins Encoded by F-Sex Factor Tra Cistrons in *Escherichia coli* Minicells. *P Natl Acad Sci USA* **76**: 4837-4841.

Bernardini ML, Mounier J, d'Hauteville H, Coquis-Rondon M & Sansonetti PJ (1989) Identification of *icsA*, a plasmid locus of *Shigella flexneri* that governs bacterial intra- and intercellular spread through interaction with F-actin. *Proc Natl Acad Sci U S A* **86**: 3867-3871.

Charles M, Perez M, Kobil JH & Goldberg MB (2001) Polar targeting of *Shigella* virulence factor IcsA in *Enterobacteriacae* and *Vibrio*. *Proc Natl Acad Sci U S A* **98**: 9871-9876.

Daniels C & Morona R (1999) Analysis of *Shigella flexneri* Wzz (Rol) function by mutagenesis and cross-linking: Wzz is able to oligomerize. *Mol Microbiol* **34**: 181-194.

Datsenko KA & Wanner BL (2000) One-step inactivation of chromosomal genes in *Escherichia coli* K-12 using PCR products. *Proc Natl Acad Sci U S A* **97**: 6640-6645.

de Boer PA, Crossley RE & Rothfield LI (1989) A division inhibitor and a topological specificity factor coded for by the minicell locus determine proper placement of the division septum in *E. coli*. *Cell* **56**: 641-649.

Egile C, d'Hauteville H, Parsot C & Sansonetti PJ (1997) SopA, the outer membrane protease responsible for polar localization of IcsA in *Shigella flexneri*. *Mol Microbiol* **23**: 1063-1073.

Egile C, Loisel TP, Laurent V, Li R, Pantaloni D, Sansonetti PJ & Carlier MF (1999) Activation of the CDC42 effector N-WASP by the *Shigella flexneri* IcsA protein promotes actin nucleation by Arp2/3 complex and bacterial actin-based motility. *J Cell Biol* **146**: 1319-1332.

Goldberg MB & Theriot JA (1995) *Shigella flexneri* surface protein IcsA is sufficient to direct actin-based motility. *Proc Natl Acad Sci U S A* **92**: 6572-6576.

Hong M & Payne SM (1997) Effect of mutations in *Shigella flexneri* chromosomal and plasmid-encoded lipopolysaccharide genes on invasion and serum resistance. *Mol Microbiol* **24**: 779-791.

Kocks C, Marchand JB, Gouin E, d'Hauteville H, Sansonetti PJ, Carlier MF & Cossart P (1995) The unrelated surface proteins ActA of *Listeria monocytogenes* and IcsA of *Shigella flexneri* are sufficient to confer actin-based motility on *Listeria innocua* and *Escherichia coli* respectively. *Mol Microbiol* **18**: 413-423.

Koppelman CM, Den Blaauwen T, Duursma MC, Heeren RM & Nanninga N (2001) *Escherichia coli* minicell membranes are enriched in cardiolipin. *J Bacteriol* **183**: 6144-6147.

Lai EM, Nair U, Phadke ND & Maddock JR (2004) Proteomic screening and identification of differentially distributed membrane proteins in *Escherichia coli*. *Mol Microbiol* **52**: 1029-1044.

Lett MC, Sasakawa C, Okada N, Sakai T, Makino S, Yamada M, Komatsu K & Yoshikawa M (1989) *virG*, a plasmid-coded virulence gene of *Shigella flexneri*: identification of the VirG protein and determination of the complete coding sequence. *J Bacteriol* **171**: 353-359.

Lima IF, Havt A & Lima AA (2015) Update on molecular epidemiology of *Shigella* infection. *Current opinion in gastroenterology* **31**: 30-37.

Lugtenberg B, Meijers J, Peters R, van der Hoek P & van Alphen L (1975) Electrophoretic resolution of the "major outer membrane protein" of *Escherichia coli* K12 into four bands. *FEBS letters* **58**: 254-258.

May KL & Morona R (2008) Mutagenesis of the *Shigella flexneri* autotransporter IcsA reveals novel functional regions involved in IcsA biogenesis and recruitment of host neural Wiscott-Aldrich syndrome protein. *J Bacteriol* **190**: 4666-4676.

Morona R & Van Den Bosch L (2003a) Lipopolysaccharide O antigen chains mask IcsA (VirG) in *Shigella flexneri*. *FEMS Microbiol Lett* **221**: 173-180.

Morona R & Van Den Bosch L (2003b) Multicopy *icsA* is able to suppress the virulence defect caused by the *wzz(SF)* mutation in *Shigella flexneri*. *FEMS Microbiol Lett* **221**: 213-219.

Morona R, van den Bosch L & Manning PA (1995) Molecular, genetic, and topological characterization of O-antigen chain length regulation in Shigella flexneri. *J Bacteriol* **177**: 1059-1068.

Morona R, Daniels C & Van Den Bosch L (2003c) Genetic modulation of *Shigella flexneri* 2a lipopolysaccharide O antigen modal chain length reveals that it has been optimized for virulence. *Microbiology* **149**: 925-939.

Niyogi SK (2005) Shigellosis. *J Microbiol* **43**: 133-143.

Pugsley AP & Buddelmeijer N (2004) Traffic spotting: poles apart. *Mol Microbiol* **53**: 1559-1562.

Purins L, Van Den Bosch L, Richardson V & Morona R (2008) Coiled-coil regions play a role in the function of the *Shigella flexneri* O-antigen chain length regulator WzzpHS2. *Microbiology* **154**: 1104-1116.

Robbins JR, Monack D, McCallum SJ, Vegas A, Pham E, Goldberg MB & Theriot JA (2001) The making of a gradient: IcsA (VirG) polarity in *Shigella flexneri*. *Mol Microbiol* **41**: 861-872.

Rokney A, Shagan M, Kessel M, Smith Y, Rosenshine I & Oppenheim AB (2009) *E. coli* transports aggregated proteins to the poles by a specific and energy-dependent process. *J Mol Biol* **392**: 589-601.

Sandlin RC, Goldberg MB & Maurelli AT (1996) Effect of O side-chain length and composition on the virulence of *Shigella flexneri* 2a. *Mol Microbiol* **22**: 63-73.

Sandlin RC, Lampel KA, Keasler SP, Goldberg MB, Stolzer AL & Maurelli AT (1995) Avirulence of rough mutants of *Shigella flexneri*: requirement of O antigen for correct unipolar localization of IcsA in the bacterial outer membrane. *Infect Immun* **63**: 229-237.

Scribano D, Petrucca A, Pompili M*, et al.* (2014) Polar Localization of PhoN2, a Periplasmic Virulence-Associated Factor of *Shigella flexneri*, Is Required for Proper IcsA Exposition at the Old Bacterial Pole. *PloS one* **9**(2): e90230

Snapper SB, Takeshima F, Anton I*, et al.* (2001) N-WASP deficiency reveals distinct pathways for cell surface projections and microbial actin-based motility. *Nat Cell Biol* **3**: 897-904.

Steinhauer J, Agha R, Pham T, Varga AW & Goldberg MB (1999) The unipolar *Shigella* surface protein IcsA is targeted directly to the bacterial old pole: IcsP cleavage of IcsA occurs over the entire bacterial surface. *Mol Microbiol* **32**: 367-377.

Stevenson G, Kessler A & Reeves PR (1995) A plasmid-borne O-antigen chain length determinant and its relationship to other chain length determinants. *FEMS Microbiol Lett* **125**: 23-30.

Suzuki T, Mimuro H, Suetsugu S, Miki H, Takenawa T & Sasakawa C (2002) Neural Wiskott-Aldrich syndrome protein (N-WASP) is the specific ligand for *Shigella* VirG among the WASP family and determines the host cell type allowing actin-based spreading. *Cell Microbiol* **4**: 223-233.

Teh MY, Tran EN & Morona R (2012) Absence of O antigen suppresses *Shigella flexneri* IcsA autochaperone region mutations. *Microbiology* **158**: 2835-2850.

Tran EN, Doyle MT & Morona R (2013) LPS unmasking of *Shigella flexneri* reveals preferential localisation of tagged outer membrane protease IcsP to septa and new poles. *PloS one* **8**(7)**:** e70508.

Tran ENH, Papadopoulos M & Morona R (2014) Relationship between O-antigen chain length and resistance to colicin E2 in *Shigella flexneri*. *Microbiol-Sgm* **160**: 589-601.

Treuner-Lange A & Sogaard-Andersen L (2014) Regulation of cell polarity in bacteria. *J Cell Biol* **206**: 7-17.

Valencia-Gallardo CM, Carayol N & Tran Van Nhieu G (2014) Cytoskeletal mechanics during *Shigella* invasion and dissemination in epithelial cells. *Cell Microbiol* 10.1111/cmi.12400.

Van den Bosch L & Morona R (2003) The actin-based motility defect of a *Shigella flexneri* *rmlD* rough LPS mutant is not due to loss of IcsA polarity. *Microb Pathog* **35**: 11-18.

Van den Bosch L, Manning PA & Morona R (1997) Regulation of O-antigen chain length is required for *Shigella flexneri* virulence. *Mol Microbiol* **23**: 765-775.

Wei J, Goldberg MB, Burland V, *et al.* (2003) Complete genome sequence and comparative genomics of *Shigella flexneri* serotype 2a strain 2457T. *Infect Immun* **71**: 2775-2786.

TABLES

Table 1: Strains and plasmids used in this study

Strain or Plasmid	Description	LPS	Source
Strain			
2457T	Wild-type *S. flexneri* 2a	S	
RMA2041	2457T *ΔicsA::Tc*^{R}	S	(Van den Bosch *et al.,* 2003)
RMA2043	2457T *ΔicsA::Tc*^{R} *ΔrmlD::Km*^{R}	R	(Van den Bosch *et al.,* 2003)
ETRM230	2457T *ΔrmlD::Km*^{R}	R	(Tran *et al.,* 2013)
MG292	2457T *minD::Km*^{R}	S	This study
Plasmids			
pBR322	medium copy number, colE1 *ori*, Ap^R, Tc^R		(Bolivar *et al.,* 1977)
pIcsA	pBR322 derivative containing cloned *icsA* gene, P_{IcsA} promoter, Ap^R		(Morona *et al.,* 2003b)
pKD4	FLP Km^R template		(Datsenko *et al.,* 2000)
pKD46	λ red recombinase, Ap^R		(Datsenko *et al.,* 2000)
pKMRM96	pGEMT::*minCDE*, Ap^R		This study
pKDMRM161	pGEMT::*minCD::Km*^{R}*E*, Ap^R		This study

Tc^R = tetracycline resistance, Km^R = kanamycin resistance, Ap^R = ampicillin resistance, S = S-LPS, R = R-LPS

FIGURE LEGENDS

Figure 1: Models of IcsA surface polarity augmentation by LPS. (A) Lateral diffusion model. It has been proposed that R-LPS *Shigellae* (without O-antigen; Oag) has a higher membrane (M) fluidity causing in IcsA (red) deposited at the pole to defuse away from the pole and down the lateral edge. (B) Model of asymmetrical masking due to O-antigen modal lengths distribution. To optimize the pathogenic role of IcsA in recruiting host actin polymerizing complexes at the pole, it is thought that LPS O-antigen chain lengths may be useful in optimizing IcsA exposure at the pole by the use of ^{S}LPS (medium blue) at the pole and ^{VL}LPS (light blue) on the lateral edges to restrict IcsA exposure. The red cross depicts the notion that LPS O-antigen chains can inhibit access of antibodies to IcsA via steric hindrance

Figure 2: Lateral and polar LPS has equivalent O-antigen modal lengths. (A) Phase micrographs of live *S. flexneri* showing wild type (2457T, top) and *minD*- phenotype (MG292, bottom). Arrowheads in the latter indicate free minicells and minicells budding from whole-cell poles. All scale bars represent 10 μm. (B) Phase micrographs of purified whole-cells and minicells from the *minD*- strain. (C) Western immunoblot analysis of standardized whole membrane samples extracted from purified whole-cells and minicells. Levels of both LPS-Oag modal length modulators $WzzB_{SF}$ and $WzzB_{pHS2}$ were assessed. Anti-IcsA served as a control that minicells were derived from polar material. (D) LPS was isolated from the standardized whole membrane samples of whole-cells and minicells from both log-phase and stationary phase cultures and analyzed by SDS-PAGE and silver staining. S = ^{S}LPS, VL = ^{VL}LPS.

Figure 3: Removal of LPS O-antigen does not change IcsA surface distribution. IcsA expression levels and surface distributions were investigated in both single *icsA* copy and

multi- *icsA* copy conditions. Panels (A – C) show data generated using wild type *S. flexneri* 2457T, *ΔicsA* (RMA2041), and *ΔrmlD* (ETRM230) strains, and panels (D – F) from strains *ΔicsA* and *ΔicsA ΔrmlD* (RMA2043) complemented with either pIcsA or base vector pBR322 (Bolivar *et al.,* 1977) (see Table 1). 'S' and 'R' denote smooth-LPS (with O-antigen) and rough-LPS (without O-antigen) respectively. Anti-IcsA Western immunoblots (A and D) show IcsA protein expression levels in total bacterial protein samples (n = 3). Chaperone DnaK served as a loading control. (B and E) Phase (top) and anti-IcsA IF micrographs (bottom) of representative bacteria. Fluorescence intensities for panels C and F are average pixel grey levels scaled equally relative to each strain. Each image is 4 µm by 4 µm. (C and F) IF experiments were repeated (n = 3-7) and IcsA surface detection (i) and surface distributions (ii) were measured for each IcsA expressing strain on a population basis. The quotients of the R-LPS and S-LPS IcsA distributions are also shown in (iii) with mean mid-cell indicated by the vertical line and red line indicating fitted linear functions (R^2 = 0.3974 and 0.8924 for C_{iii} and F_{iii} respectively). OP = old pole, MNP = mean new pole, ns = not significant. Differences in mean surface detection for (i) were analyzed by two-tailed t-test, and differences in distribution between OP, MNP and mid-cell in (iii) analyzed by one-way ANOVA (** = $p < 0.01$, *** = $p < 0.001$, **** = $p < 0.0001$).

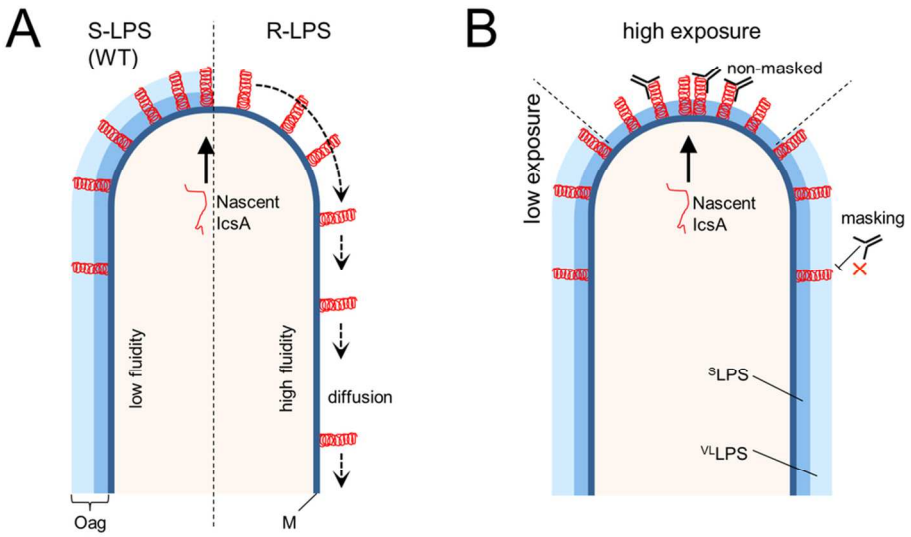

Figure 1: Models of IcsA surface polarity augmentation by LPS (2x final width and hight)

(A) Lateral diffusion model. It has been proposed that R-LPS *Shigellae* (without O-antigen; Oag) has a higher membrane (M) fluidity causing in IcsA (red) deposited at the pole to defuse away from the pole and down the lateral edge. (B) Model of asymmetrical masking due to O-antigen modal lengths distribution. To optimize the pathogenic role of IcsA in recruiting host actin polymerizing complexes at the pole, it is thought that LPS O-antigen chain lengths may be useful in optimizing IcsA exposure at the pole by the use of ^{S}LPS (medium blue) at the pole and ^{VL}LPS (light blue) on the lateral edges to restrict IcsA exposure. The red cross depicts the notion that LPS O-antigen chains can inhibit access of antibodies to IcsA via steric hindrance.
95x57mm (300 x 300 DPI)

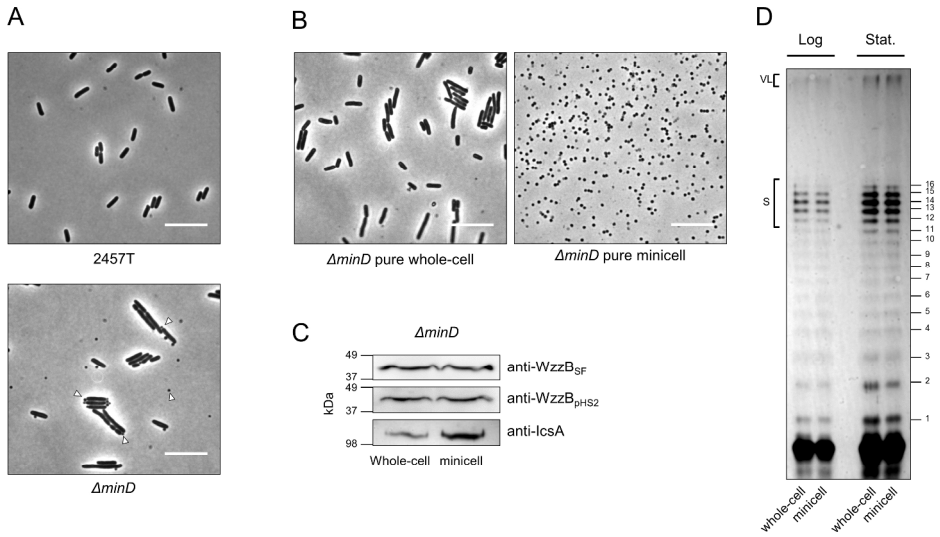

Figure 2: Lateral and polar LPS has equivalent modal lengths (2x final width and hight)

(A) Phase micrographs of live *S. flexneri* showing wild type (2457T, top) and *minD*- phenotype (MG292, bottom). Arrowheads in the latter indicate free minicells and minicells budding from whole-cell poles. All scale bars represent 10 µm. (B) Phase micrographs of purified whole-cells and minicells from the *minD*- strain. (C) Western immunoblot analysis of standardized whole membrane samples extracted from purified whole-cells and minicells. Levels of both LPS-Oag modal length modulators $WzzB_{SF}$ and $WzzB_{pHS2}$ were assessed. Anti-IcsA served as a control that minicells were derived from polar material. (D) LPS was isolated from the standardized whole membrane samples of whole-cells and minicells from both log-phase and stationary phase cultures and analyzed by SDS-PAGE and silver staining. S = ^{S}LPS, VL = ^{VL}LPS.
336x200mm (232 x 232 DPI)

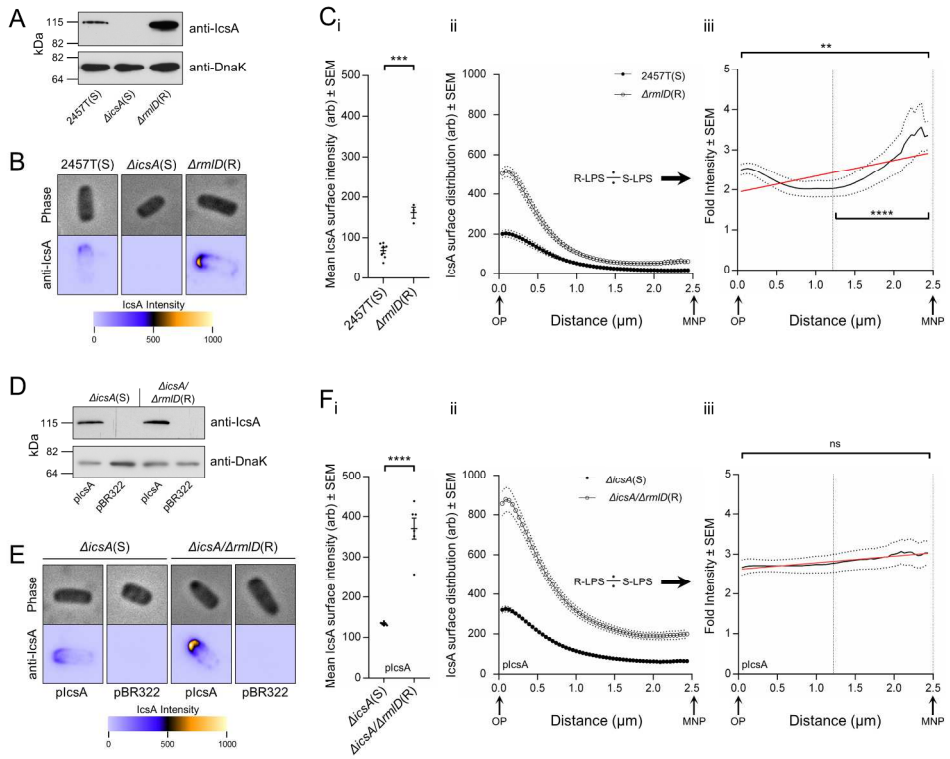

Figure 3: Removal of LPS O-antigen does not change IcsA surface distribution (2x final width and hight)

IcsA expression levels and surface distributions were investigated in both single icsA copy and multi- icsA copy conditions. Panels (A – C) show data generated using wild type *S. flexneri* 2457T, ΔicsA (RMA2041), and *ΔrmlD* (ETRM230) strains, and panels (D – F) from strains *ΔicsA* and *ΔicsA ΔrmlD* (RMA2043) complemented with either pIcsA or base vector pBR322 (Bolivar et al., 1977) (see Table 1). 'S' and 'R' denote smooth-LPS (with O-antigen) and rough-LPS (without O-antigen) respectively. Anti-IcsA Western immunoblots (A and D) show IcsA protein expression levels in total bacterial protein samples (n = 3). Chaperone DnaK served as a loading control. (B and E) Phase (top) and anti-IcsA IF micrographs (bottom) of representative bacteria. Fluorescence intensities for panels C and F are average pixel grey levels scaled equally relative to each strain. Each image is 4 μm by 4 μm. (C and F) IF experiments were repeated (n = 3-7) and IcsA surface detection (i) and surface distributions (ii) were measured for each IcsA expressing strain on a population basis. The quotients of the R-LPS and S-LPS IcsA distributions are also shown in (iii) with mean mid-cell indicated by the vertical line and red line indicating fitted linear functions (R2 = 0.3974 and 0.8924 for C_{iii} and F_{iii} respectively). OP = old pole, MNP = mean new pole, ns = not significant. Differences in mean surface detection for (i) were analyzed by two-tailed t-test, and differences in distribution between OP, MNP and mid-cell in (iii) analyzed by one-way ANOVA (** = $p < 0.01$, *** = $p < 0.001$, **** = $p < 0.0001$).

336x273mm (232 x 232 DPI)

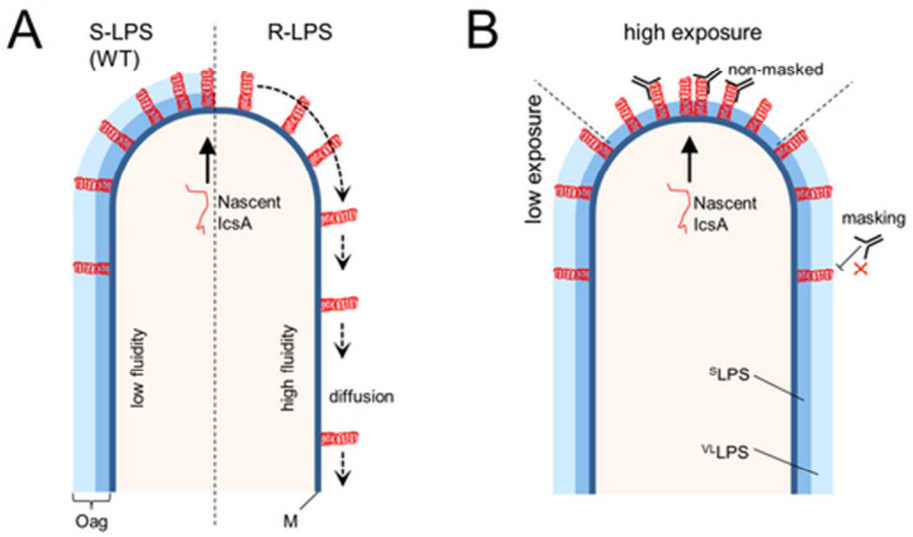

48x28mm (300 x 300 DPI)